

A COMPARATIVE STUDY ON SQUARE AND CIRCULAR HIGH STRENGTH CONCRETE-FILLED STEEL TUBE COLUMNS

S. Guler^{1,*}, A. Çopur² and M. Aydoğan³

¹ PhD, Department of Civil Engineering, Istanbul Technical University, Istanbul, Turkey

² MSc, Department of Civil Engineering, Istanbul Technical University, Istanbul, Turkey

³ Professor, Department of Civil Engineering, Istanbul Technical University, Istanbul, Turkey

*(Corresponding author: E-mail: : gulersoner@yandex.com)

Received: 19 December 2012; Revised: 5 February 2013; Accepted: 28 February 2013

ABSTRACT: This paper investigates the behavior of axially loaded square and circular high strength concrete-filled steel tube (CFST) columns. The effects of steel tube thickness and bond strength between the steel tube and the concrete core on axial load capacity and ductility are studied. The performance indices named ductility index (DI), strength enhancement index (SI) and concrete contribution ratio (CCR) are also evaluated for the square and the circular high strength CFST columns. The experimental results are compared with the values estimated by current design codes such as Eurocode 4 (EC4) and AISC-LRFD (1999). The results show that the difference of the axial load capacity due to loss of bonding is significant for both of the square and the circular high strength CFST columns. However, this difference is equal for both of the square and the circular columns with H/t or D/t smaller than 20. The EC4 design code, contrary to the AISC-LRFD (1999), generally overestimates the axial load capacity of the square and the circular high strength CFST columns.

Keywords: High strength concrete, concrete-filled steel tube stub columns, axial load capacity, D/t ratio, bond effect, design codes, performance indices

1. INTRODUCTION

Concrete-filled steel tube (CFST) columns are widely used in the construction of high-rise buildings, bridges, subway platforms, and barriers. The CFST columns provide excellent static and earthquake-resistant properties such as high strength, high ductility, high stiffness, and large energy-absorption capacity. The CFST columns provide some advantages of both steel and concrete. The steel tube assists to carry the axial load and confines the concrete core. Furthermore, the steel tube annihilates the permanent formwork, which reduces construction time, while the concrete core takes the axial load and avoids or delays local buckling of the steel tube (Lu and Zhao [1]).

Recently, there is an increase in use of high strength concrete (HSC) in major construction projects such as high-rise buildings, offshore oil platforms and bridges. HSC is known as a material that is generally associated with low water to cement ratio, high durability, low permeability and a high compressive strength in the range of over 60 MPa. In the recent years using chemical admixtures and silica fumes that partially replace cement as well as applying improved design methods and mixing techniques allows the engineers to produce concrete with much higher compressive strength. Concrete with a compressive strength over 100 MPa can be easily produced commercially using conventional methods and materials. As a result, today HSC has much better performance compared to normal strength concrete. That is why it is commonly used in the construction practice in many countries all over the world (Shah and Ribakov [2]).

One of the major concerns related to HSC is the need of sufficient confinement. Poisson ratio is slightly less and the amount of shrinkage is higher of HSC compared with low and normal strength concrete. Because of those effects, the confining effect of the steel tube to the high strength concrete is not as much as the low and normal strength concrete. Hence, the difference of the axial

load capacity due to loss of bonding is critical for high strength CFST columns. There are many studies to investigate the bond effect for CFST columns with concrete compressive strength up to 100 MPa. Roeder et al. [3] investigate that the importance of bond stress and interface conditions on the axial load capacities of the circular CFST columns with concrete compressive strength varies from 28.6 MPa to 47.2 MPa. The test results show that the bond capacity, for the circular CFST columns, is smaller with large diameter tubes and large diameter-to thickness (D/t) ratios. An experimental study is conducted on circular high strength CFST columns with cylinder concrete strength of 65 MPa by (Johansson and Gylltoft [4]). The test results imply that the bond strength has no influence on the behavior when the steel and concrete sections are loaded simultaneously. On the contrary, for the columns with the load applied only to the concrete section, the bond strength highly affected the confinement effects and, consequently, the mechanical behavior of the columns. Giakoumelis and Lam [5] examine 15 circular CFST columns with concrete compressive strength of 30, 60, and 85 MPa. Contrary to the results of Johansson and Gylltoft [4], the results reveal that the difference of the axial load capacity due to loss of bonding is negligible for low or normal concrete strength while it is critical for the high strength concrete. The difference of the axial load capacity for the high strength CFST columns is 17%. Although there are lots of studies on CFST columns with concrete compressive strength up to 100 MPa, there still needs further analyses on the CFST columns with concrete strength over 100 MPa. To fill such a gap in the literature, Guler et al. [6] study the bond effect on the behavior of the square high strength CFST columns with concrete compressive strength of 115 MPa depending on the different steel tube thickness. The test results clearly show that the difference of the axial load capacity due to loss of bonding is significant for the square high strength CFST columns. The biggest difference of the axial load capacity is 14% for the square high strength CFST columns with 3 mm steel tube thickness.

1.1 Objective

The first aim of this study is to compare the difference of the axial load capacity due to the bond effect for the square and the circular high strength CFST columns with concrete strength over 100 MPa depending on the different steel tube thickness. Secondly, some important parameters the ductility index (DI), the strength enhancement index (SI) and the concrete contribution ratio (CCR) are compared and evaluated for the square and the circular high strength CFST columns. Finally, the axial load capacities of the high strength CFST columns are compared with the values predicted by the EC4 [7]; the American Institute of Steel Construction- Load Resistance Factor Design AISC-LRFD [8] design codes.

2. EXPERIMENTAL PROGRAM

Totally, 40 the square and the circular high strength CFST columns are tested under monotonic axial compression. The steel tube and the concrete are simultaneously loaded. To achieve this, the steel plates with thickness of 10 mm are welded top and bottom surfaces of the square and the circular CFST columns. The specimens are separated as greased and non-greased specimens to investigate the bond effect depending on the different steel tube thickness. The nominal steel tube thickness of the specimens is selected 3 mm, 4 mm, and 5 mm for the square columns and 3 mm, 4 mm, and 6 mm for the circular ones. The height-to-thickness (H/t) ratio of the square columns and diameter-to-thickness ratio (D/t) ratio of the circular columns vary from 19 to 37.9. All the specimens are 400 mm in length to prevent the slenderness effect and to ensure that the specimens behave as stub columns. A thin layer of non-shrinkage cementitious mortar is poured on the top surface of the concrete to provide the concrete core and the steel tube are loaded simultaneously. All the tests are performed three months after casting of concrete. The square and the circular specimens before concrete-filled are shown in Figure 1.



Figure 1. The Square and Circular Column Specimens before Concrete Filled

2.1 Concrete Properties

A batch of concrete is mixed for this study. The regular CEM I PÇ 42.5R is used as cement material in the mix. Dramix ZP 305 steel fibers with hooked ends are used in the mix at two percent (2%) by volume. The fibers in the mix have a diameter of 0.55 mm, length of 30 mm, and tensile strength of 1100 MPa. Standard cylindrical (150 mm x 300 mm) concrete samples are tested in accordance to Turkish Standard TS EN 206 [9] and TS EN 12390 [10] to determine the compressive strength. The average compressive strengths of the concrete (f_{cm}) at the time of test are 115 MPa for cylindrical samples. Cylindrical samples are tested at a loading rate of 250 kN / min. Water-binder (cement + silica fume) ratio is kept constant at 0.13. The typical mix composition of the high strength concrete is given in Table 1.

Table 1. High Strength Concrete Composition

Mix proportions kg (for 1 m ³ concrete)							
Cement	Siliceous Sand (0.5-2mm)	Siliceous Powder (0-0.5mm)	Silica fume	Super Plasticizer	Water	ZP305 Dramix steel fiber	Total
1000	325	500	250	30	165	160	2430

2.2 Steel Properties

All the steel tubes are manufactured from mild steel. In order to determine the actual material properties, three coupons are cut from each steel tube with different steel tube wall for the square and the circular specimens according to Turkish Standard TS 138 EN 10002 [11]. The average yield stress, tensile strength, and modulus of elasticity for the square and the circular specimens are given in Table 2.

Table 2. The Material Properties of the Steel Tubes Obtained from the Coupon Tests

	f_y (MPa)	f_u (MPa)	E_s (MPa)
Square 3 mm	300	369	200000
Square 4 mm	304	375	200000
Square 5 mm	310	383	200000
Circular 3 mm	311	400	200000
Circular 4 mm	306	389	200000
Circular 6 mm	314	418	200000

2.3 Test Setup

All the tests are performed at the Istanbul Technical University, Civil Engineering Department in Structure and Earthquake Laboratory. Testing of the square and the circular high strength CFST stub columns are tested using a 5000 kN capacity INSTRON testing machine. Two linear variable differential transducers (LVDTs) are placed at diametrically opposite positions to measure the axial deformation. Four strain gauges are used for each specimen to measure strains at the middle height, two strain gauges at the top and two strain gauges at the bottom. The data is acquired at each 30 kN load until the yield point. After this point, data is sampled at 10 kN intervals. The test setup is shown in Figure 2a, 2b and Figure 3a, 3b.

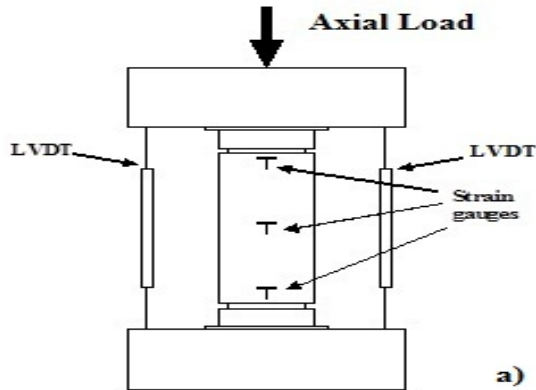
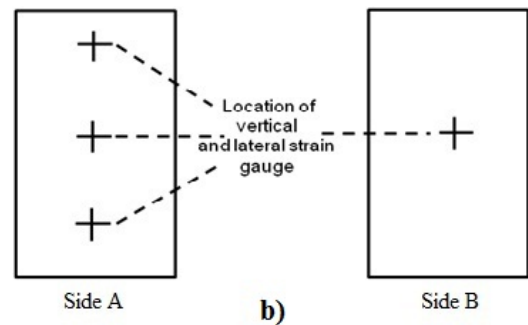


Figure 2a. The Schematic View of Test Set Up



2b. Location of Strain Gauges



Figure 3a. The Test Setup for the Circular Columns



3b. The Test Setup for the Square Columns

The specimens filled with concrete are labeled according to their shape, thickness of steel tube, greased or non-greased and their order. For instance, S3G-1, denotes that the specimen is square (S), the steel tube has a thickness of 3 mm, the specimen is greased (G), and it is the first specimen in this group. Similarly, C5NG-2, denotes that the specimen is circular (C), the steel tube has a thickness of 5 mm, the specimen is non-greased (NG), and it is the second specimen in this group. The square and the circular hollow specimens (unfilled concrete) were labeled similarly except the greased or the non-greased label. The test properties and the axial load capacities (N_{ue}) obtained from the tests of the square and the circular specimens are given in Table 3 and Table 4, respectively.

3. EXPERIMENTAL RESULTS

3.1 Loads versus Axial Shortening

Axial load – axial shortening curves for the square and the circular specimens are shown in Figures 4. As seen in these figures, all the square and the circular high strength CFST columns have no obvious axial shortening during the initial linear elastic period of the loading process, which is the cooperation of steel tube and the concrete core. When the axial load reaches about 90 to 95% of the peak load, the steel tube starts yielding, micro-cracking is initiated and propagated in concrete core, and the local buckling slightly occurs. Therefore, the axial and lateral strains measured at mid-height start to increase notably. The axial load of the square and the circular high strength CFST columns rapidly decrease after the peak load with increased axial shortenings.

As expected, the difference of the axial load capacity is much higher for the circular columns than the square ones with same steel tube wall. However, the difference of the axial load capacity is gradually reduced when the steel tube wall is increased and same for both of the square and the circular high strength CFST columns with H/t or D/t ratio smaller than 20. As seen from Figures 4, it can be clearly said that the bond effect on the axial load capacity is more and more reduced for the square and the circular high strength CFST columns with H/t or D/t ratio smaller than 20. The difference of the average axial load capacity between the greased and the non-greased square and circular high strength CFST columns is shown in Figure 4, Figure 5, and Figure 6.

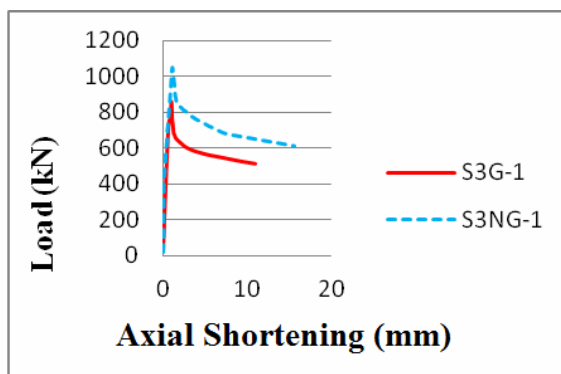
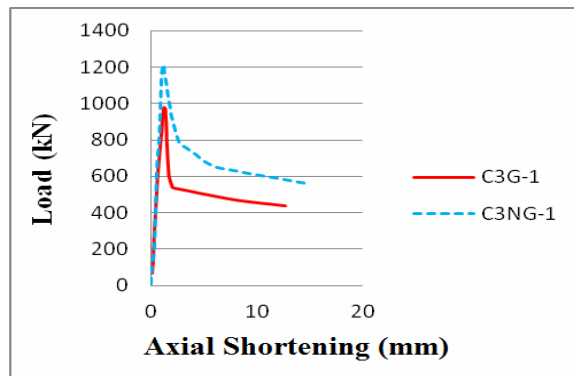
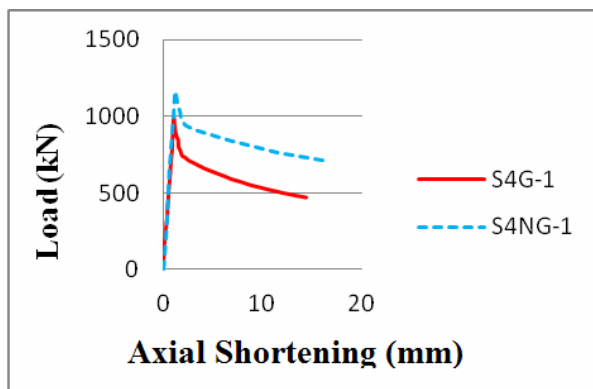


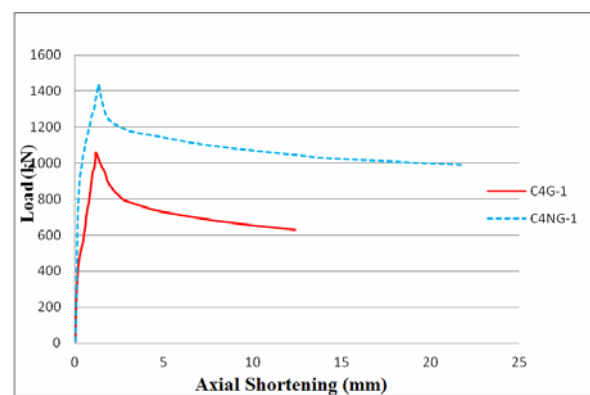
Figure 4a. The Square Columns with 3mm Steel Tube Wall



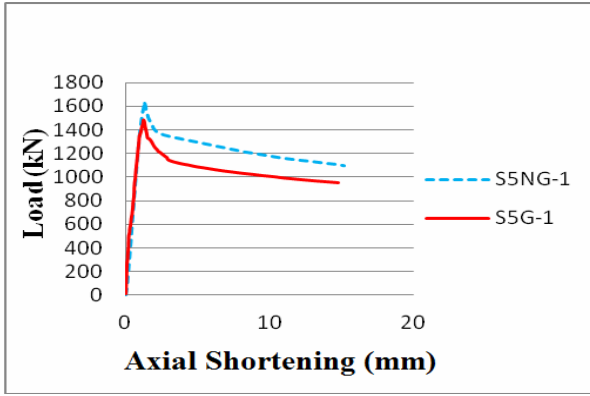
b. The Circular Columns with 3mm Steel Tube Wall



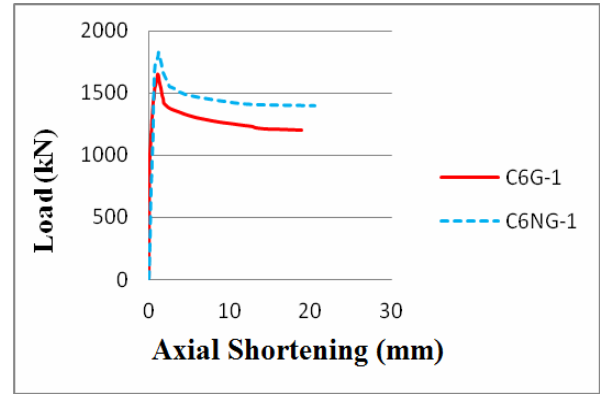
c. The Square Columns with 4 mm Steel Tube Wall



d. The Circular Columns with 4 mm Steel Tube Wall



e. The Square Columns with 5 mm Steel Tube Wall



f. The circular columns with 6 mm steel tube wall

Table 3. Measured Square Specimen Results

Specimen	H x B x t (mm)	L (mm)	H/t	f _{cm} (MPa)	f _y (MPa)	A _s (mm ²)	A _c (mm ²)	N _{ue} (kN)
S3G-1	100.08 x 99.86 x 3.01	400	33.2	115	300	1167	8827	856
S3G-2	100.06 x 99.91 x 3.02	400	33.1	115	300	1171	8826	920
S3G-3	100.06 x 99.93 x 3.01	400	33.2	115	300	1168	8831	902
S3NG-1	100.08 x 100.05 x 3.03	400	33	115	300	1176	8837	1049
S3NG-2	100.07 x 100.06 x 3.02	400	33.1	115	300	1172	8841	1017
S3H-1	99.89 x 99.95 x 3.02	400	33.1	-	300	1171	-	295
S3H-2	99.91 x 99.97 x 3.02	400	33.1	-	300	1171	-	322
S4G-1	100.12 x 100.21 x 3.97	400	25.2	115	304	1528	8505	990
S4G-2	100.06 x 100.08 x 3.99	400	25.1	115	304	1533	8481	980
S4NG-1	101.05 x 101.23 x 3.98	400	25.4	115	304	1547	8683	1160
S4NG-2	101.03 x 101.08 x 4.01	400	24.9	115	304	1556	8656	1100
S4H-1	99.96 x 99.87 x 4.02	400	24.9	-	304	1542	-	442
S4H-2	99.95 x 99.84 x 4.01	400	24.9	-	304	1538	-	460
S5G-1	100.02 x 101.04 x 4.98	400	20.1	115	310	1903	8201	1481
S5G-2	100.05 x 101.23 x 4.97	400	20.1	115	310	1902	8226	1474
S5NG-1	100.11 x 100.16 x 5.02	400	19.9	115	310	1910	8117	1642
S5NG-2	100.17 x 100.21 x 4.97	400	20.2	115	310	1893	8145	1636
S5H-1	99.97 x 99.88 x 5.05	400	19.8	-	310	1916	-	685
S5H-2	99.96 x 99.87 x 5.02	400	19.9	-	310	1905	-	712

Table 4. Measured Circular Specimen Results

Specimen	D x t (mm)	L (mm)	D/t	f _{cm} (MPa)	f _y (MPa)	A _s (mm ²)	A _c (mm ²)	N _{ue} (kN)
C3G-1	114.24 x 3.02	400	37.8	115	311	1055	9190	980
C3G-2	114.21 x 3.02	400	37.8	115	311	1054	9185	909
C3G-3	114.19 x 3.01	400	37.9	115	311	1051	9185	940
C3NG-1	114.26 x 3.02	400	37.8	115	311	1055	9194	1214
C3NG-2	114.23 x 3.02	400	37.8	115	311	1055	9188	1233
C3H-1	114.21 x 3.03	400	37.7	-	311	1058	-	402
C3H-2	114.24 x 2.99	400	38.2	-	311	1044	-	416
C4G-1	114.18 x 3.98	400	28.6	115	306	1377	8857	1060
C4G-2	114.22 x 3.99	400	28.7	115	306	1381	8860	1221
C4G-3	114.27 x 3.98	400	28.5	115	306	1378	8872	1116
C4NG-1	114.29 x 4.01	400	28.5	115	306	1389	8865	1436
C4NG-2	114.26 x 4.02	400	28.4	115	306	1392	8857	1315
C4NG-3	114.23 x 4.01	400	28.5	115	306	1388	8855	1420
C4H-1	114.27 x 4.02	400	28.4	-	306	1392	-	624
C4H-2	114.25 x 4.01	400	28.5	-	306	1388	-	642
C6G-1	114.21 x 5.99	400	19.1	115	314	2035	8204	1650
C6G-2	114.28 x 5.98	400	19.1	115	314	2034	8219	1615
C6NG-1	114.32 x 5.98	400	19.1	115	314	2034	8225	1830
C6NG-2	114.33 x 5.98	400	19.1	115	314	2035	8226	1810
C6H-1	114.28 x 6.02	400	19	115	314	2046	-	832
C6H-2	114.27 x 6.02	400	19	115	314	2046	-	850

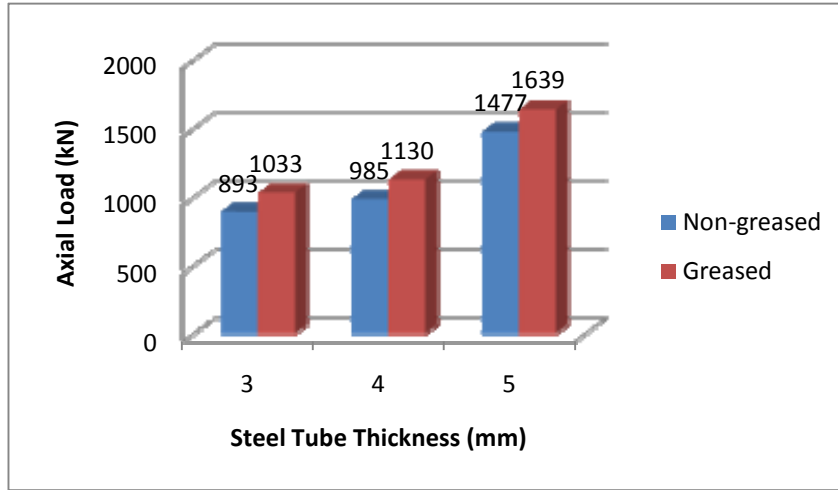


Figure 5. The Difference of the Average Axial Load Capacity for the Greased and the Non-greased Square Specimens

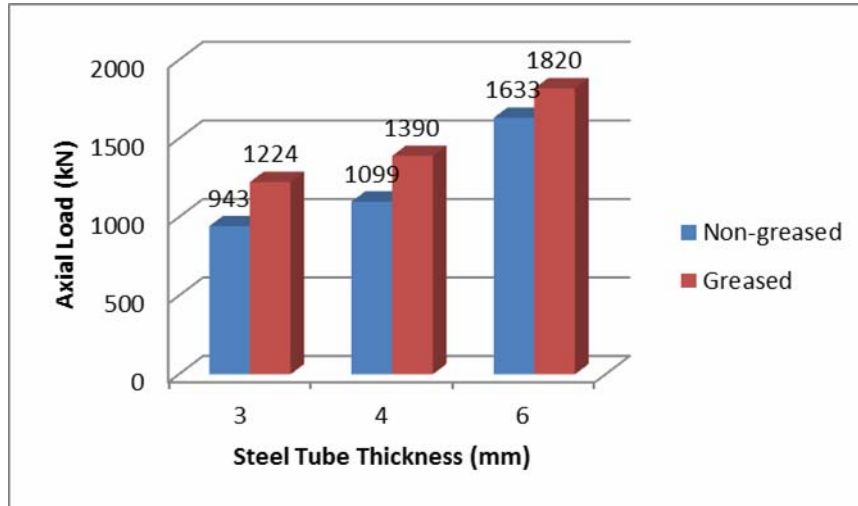


Figure 6. The Difference of the Average Axial Load Capacity for the Greased and the Non-greased Circular Specimens

3.2 Performance Indices

Some important parameters are defined to compare the ductility and the strength enhancement of the CFST columns by Han et al. [12]; and Yang et al. [13]. Those parameters are the ductility index (DI), the strength enhancement index (SI), and the concrete contribution ratio (CCR). They are defined from Eq.1 to Eq.3.

$$DI = \frac{\delta_{85\%}}{\delta_u} \quad (1)$$

$$SI = \frac{N_{u, \text{filled}}}{A_s f_y + A_c f_{ck}} \quad (2)$$

$$CCR = \frac{N_{u, \text{filled}}}{N_{u, \text{hollow}}} \quad (3)$$

Here, $N_{u, \text{filled}}$ is the ultimate load reached in the tests; $N_{u, \text{hollow}}$ is the ultimate load of the un-filled steel tubes; δ_u is the axial shortening at the ultimate load; $\delta_{85\%}$ is the axial shortening when the load falls to 85% of the ultimate load; A_s and A_c is the cross-sectional area of the steel tube and the concrete, respectively; f_y and f_{ck} is the yielding stress of the steel tube and the characteristic compressive strength of the concrete, respectively.

The ductility of the specimens is assessed in terms of the ductility index (DI) depicted in Eqn.1. The strength enhancement index (SI) can be described as the ratio the axial load capacity of the composite section to the sum of the strengths of the steel tube and the concrete core. The level of strength enhancement arising from the concrete filling is represented by the CCR that is defined as the ratio the maximum load of composite column to the hollow column. The relationships between the constraining factor and the ductility index, strength enhancement index and the concrete contribution ratio are shown in Figures 6.

As seen from Figures 7 and Table 5, there is a significant increase in the DI when the D/t ratio is reduced for both of the square and the circular CFST columns. However, the increase in the DI is notably higher for the circular CFST columns than the square ones. The average increase in the DI for the square and the circular columns, compared with the 3 mm and 5 mm and 6 mm steel tube wall, is 29% and 63%, respectively. This proves that when the D/t ratio of both of the high strength CFST columns is reduced, the circular high strength CFST columns significantly exhibit more ductile behavior than the square ones after the peak load. Similarly, there is a significant increase in the SI when the H/t or D/t ratio of the square and the circular high strength CFST columns is reduced. However, the increase in the SI is only valid for the square and the circular CFST columns with 5 mm and 6 mm steel tube wall. As seen, there is no any enhancement in the SI for the thinner (3 mm and 4 mm) CFST columns. Compared with the increase in the DI, the increase in the SI is slightly larger for the circular columns than the square ones. The average increase in the SI for the square and the circular high strength CFST columns, compared with the 3 mm and 5 mm or 6 mm steel tube wall, is 38% and 48%, respectively. Contrary to the DI and the SI performance indices, the CCR performance indices that represent the benefit of concrete filling into the hollow steel tube is much more critical for the square high strength CFST columns than the circular ones. The average increase in the CCR for the square and the circular columns, steel tube wall is reduced from 6 mm or 5 mm to 3 mm, 41% and 22%, respectively. This is due to fact that the square hollow steel tubes are more vulnerable to local buckling and has significantly smaller axial load capacities than the circular ones. Furthermore, compared with the same steel tube wall, the non-greased square and the circular CFST columns have higher performance indices than the greased ones due to stronger bond effect between the steel tube and the concrete core.

Table 5. Values of Performance Indices

Specimen	DI	SI	CCR	Specimen	DI	SI	CCR
S3G-1	1.28	0.62	2.74	C3G-1	1.39	0.71	2.08
S3G-2	1.32	0.67	2.95	C3G-2	1.36	0.66	1.93
S3G-3	1.3	0.66	2.89	C3G-3	1.38	0.68	2.00
S3NG-1	1.41	0.77	3.36	C3NG-1	1.42	0.88	2.58
S3NG-2	1.38	0.74	3.26	C3NG-2	1.46	0.89	2.62
S4G-1	1.51	0.69	2.36	C4G-1	1.67	0.74	1.68
S4G-2	1.49	0.68	2.33	C4G-2	1.7	0.85	1.93
S4NG-1	1.61	0.8	2.76	C4G-3	1.69	0.77	1.77
S4NG-2	1.58	0.76	2.62	C4NG-1	1.79	0.99	2.27
S5G-1	1.71	0.98	2.08	C4NG-2	1.81	0.91	2.08
S5G-2	1.69	0.97	2.07	C4NG-3	1.83	0.98	2.25
S5NG-1	1.74	1.09	2.31	C6G-1	2.23	1.05	1.79
S5NG-2	1.78	1.08	2.30	C6G-2	2.21	1.03	1.75
				C6NG-1	2.38	1.17	1.98
				C6NG-2	2.36	1.16	1.96

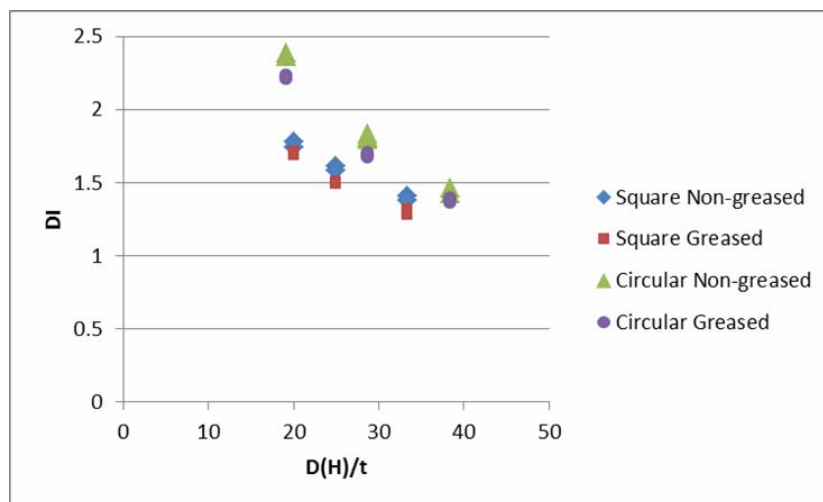


Figure 7a. DI versus D (H)/t Relationship

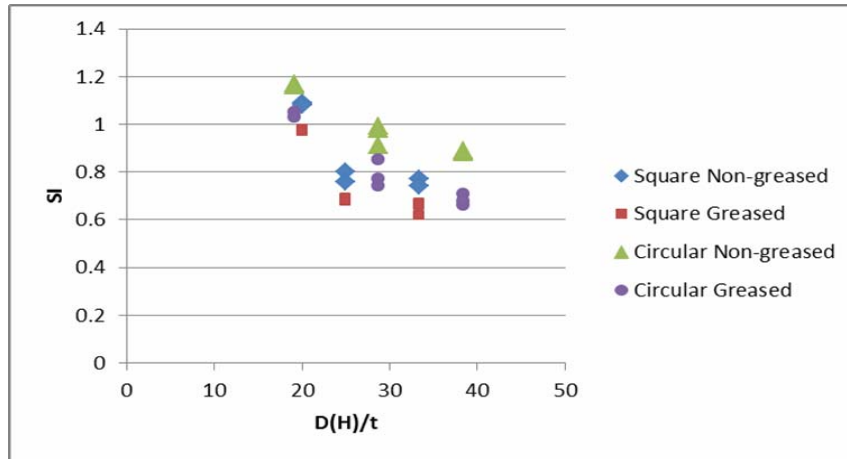


Figure 7b. SI versus D(H)/t Relationship

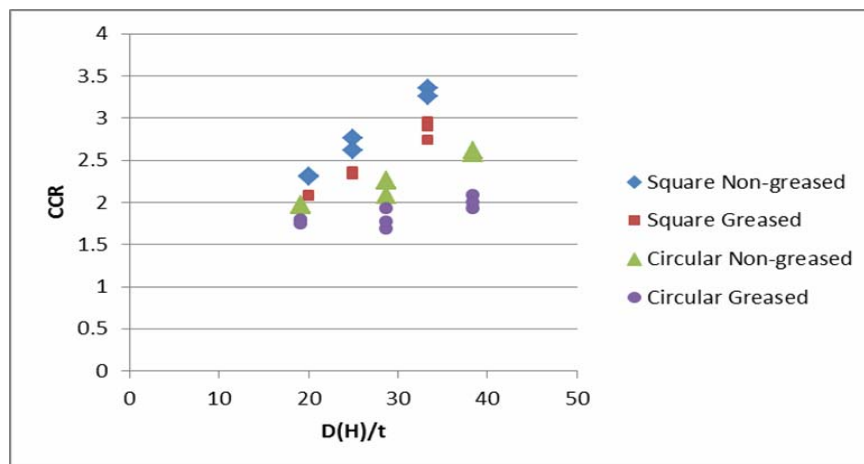


Figure 7c. CCR versus D(H)/t Relationship

4. DESIGN CODES

4.1 Eurocode 4:

The EC4 (2004) design code is the most lately completed international standard in composite construction. EC4 covers concrete encased and partially encased steel sections and concrete-filled sections with or without reinforcement. The EC4 approach is limited to CFST columns with concrete strength of 50 MPa. The axial load capacity of the square CFST columns according to the EC4 is given by Eq. 4:

$$N_{u,EC4} = A_c f_{ck} + A_s f_y \tag{4}$$

The EC4 takes account the confining effect by the steel tube calculating the axial load capacity of the circular CFST columns. If the relative slenderness does not exceed 0.5 and e/D is smaller than 0.1, the axial load capacity of the circular CFST columns can be calculated from Eq.5 to 11:

$$N_{u,EC4} = \left(1 + \eta_c \frac{t}{D} \frac{f_y}{f_{ck}} \right) f_{ck} A_c + \eta_a f_y A_s \tag{5}$$

$$\eta_c = 4.9 - 18.5\lambda + 17\lambda^2 \quad (\eta_c \geq 0) \quad (6)$$

$$\eta_a = 0.25(3 + 2\lambda) \quad (\eta_a \leq 1) \quad (7)$$

$$\lambda = \sqrt{\frac{N_{pl,R}}{N_{cr}}} \leq 0.5 \quad (8)$$

$$N_{pl,R} = A_c f_{ck} + A_s f_y \quad (9)$$

$$N_{cr} = \frac{\pi^2 (EI)_e}{l^2} \quad (10)$$

$$(EI)_e = A_s E_s + 0.6 E_{cm} A_c \quad (11)$$

Here, η_c is the coefficient of confinement for the concrete; η_a is the coefficient of confinement for the steel tube; λ is the relative slenderness; l is the buckling length of the CFST column; E_{cm} is the secant elastic modulus of concrete; $(EI)_e$ is the effective flexural stiffness; f_{ck} is the characteristic concrete cylinder strength; and f_y is the yield strength of the steel.

As seen from Table 6 and Figure 8, although the EC4 overestimate the axial load capacity for the square and the circular high strength CFST columns with thinner steel tube wall (especially nominal D/t or H/t is greater than 33), it can reliably predict the axial load capacity for the square and the circular high strength CFST columns with nominal D/t or H/t ratio smaller than 20. In addition, due to loss of bonding and little confinement by the steel tubes, the axial load capacity of greased the square and the circular high strength CFST columns obtained from test results, compared with the non-greased columns, are lower than the values predicted by the EC4. This difference is much greater for the columns with the thinner steel tube wall than the thicker ones. Furthermore, the EC4 is more conservative for the square high strength CFST columns than the circular ones. This is due to the fact that although the EC4 take account the confinement effect of the steel tube to the concrete core for the circular high strength CFST columns, it doesn't consider the confinement effect for the square ones. The average $N_{ue} / N_{u,EC4}$ for greased the square and the circular CFST columns is 0.75 and 0.62, respectively. In addition, the average $N_{ue} / N_{u,EC4}$ for non-greased the square and the circular columns is 0.87 and 0.79, respectively.

4.2 AISC-LRFD

The axial load capacity of the square and the circular CFST columns according to AISC-LRFD (1999) design code is given from Eq.12 to Eq.16:

$$F_{my} = f_y + 0.85 f_c (A_c / A_s) \quad (12)$$

$$E_m = E_s + 0.4 E_c (A_c / A_s) \quad (13)$$

$$\lambda_c = \frac{KL}{\pi r_m} \sqrt{\frac{F_{my}}{E_m}} \quad (14)$$

$$F_{cr} = 0.658^{\lambda_c^2} F_{my} \tag{15}$$

$$N_u = A_s F_{cr} \tag{16}$$

As seen From Table 6 and Figure 9, it can be said that the AISC-LRFD, similarly EC4, is not safe for the square and the circular columns with the thinner steel tube wall compared to the thicker ones. The average N_{ue} / N_u , AISC-LRFD for the greased square and the circular columns is 0.97 and 1.05, respectively. In addition, the average N_{ue} / N_u , AISC-LRFD for the non-greased square and the circular columns is 1.12 and 1.28, respectively. The axial load capacities obtained from the test results for the square and the circular high strength CFST columns are compared with the values predicted by the EC4 and the AISC-LRFD is given in Table 7, Figure 8, and Figure 9.

Table 6. Comparisons of Axial Load Capacities between Test Results and Design Codes

Specimen No	N_{ue} (kN)	$N_{ue}/N_u, EC4$	$N_{ue}/N_u, AISC$	Specimen No	N_{ue} (kN)	$N_{ue}/N_u, EC4$	$N_{ue}/N_u, AISC$
S3G-1	856	0.63	0.82	C3G-1	980	0.59	0.93
S3G-2	920	0.67	0.88	C3G-2	909	0.55	0.87
S3G-3	902	0.66	0.87	C3G-3	940	0.56	0.90
S3NG-1	1049	0.77	1.00	C3NG-1	1214	0.73	1.16
S3NG-2	1017	0.74	0.97	C3NG-2	1233	0.74	1.17
S4G-1	990	0.69	0.88	C4G-1	1060	0.59	0.96
S4G-2	980	0.68	0.88	C4G-2	1221	0.68	1.10
S4NG-1	1160	0.79	1.02	C4G-3	1116	0.62	1.01
S4NG-2	1100	0.75	0.97	C4NG-1	1436	0.80	1.29
S5G-1	1481	0.97	1.23	C4NG-2	1315	0.73	1.18
S5G-2	1474	0.96	1.22	C4NG-3	1420	0.79	1.28
S5NG-1	1642	1.08	1.37	C6G-1	1650	0.79	1.32
S5NG-2	1636	1.07	1.37	C6G-2	1615	0.77	1.29
Mean		0.8	1.04	C6NG-1	1830	0.88	1.46
St.Dev.		0.15	0.19	C6NG-2	1810	0.87	1.45
				Mean		0.71	1.16
				St. Dev.		0.11	0.19

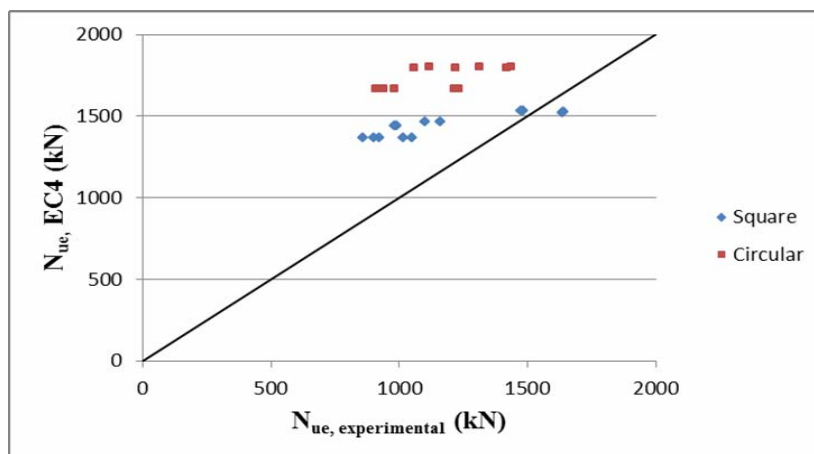


Figure 8. Comparison of test results with EC4

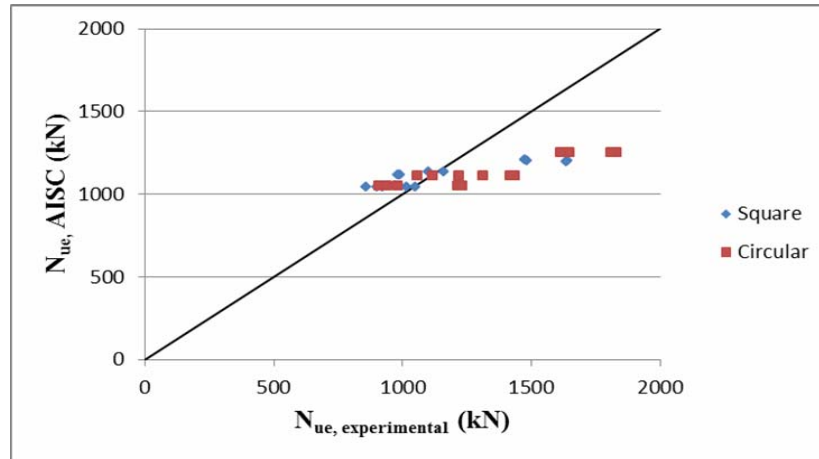


Figure 9. Comparison of Test Results with AISC-LRFD

5. CONCLUSIONS

The present study is an attempt to investigate the bond effect on axial load capacity and performance indices of axially loaded the square and the circular high strength CFST columns with regard to different steel tube thickness. The test results are also compared with the results of present design codes such as the EC4 and the AISC-LRFD. The main conclusions obtained from this study can be drawn as below:

As known, plastic, autogenous, and drying shrinkage of high strength concrete is higher than low and normal strength concrete. As a result of this, the bond stresses between the steel tube and the concrete core is weaker for the high strength CFST columns than the low and normal strength CFST columns. Thus, the reduction on the axial load capacity due to loss of bonding is not negligible for both of the square and the circular high strength CFST columns. Furthermore, the circular high strength CFST columns have higher bond stress capacity than the square ones. As a result of this study, the $D(H)/t$ ratio of 20 may be considered as a separation point for the bond effect on the axial load capacity of the square and the circular high strength CFST columns. The biggest difference of the axial load capacity for the circular and the square high strength CFST columns is 23% and 14%, respectively.

To decrease the $D(H)/t$ ratio significantly improves the ductility performance of the square and the circular high strength CFST columns. However, there is no much benefit to enhance the axial load capacity of the square and the circular high strength CFST columns. Hence, enhancement in ductility is more pronounced than gain in axial load capacity for both of the square and the circular high strength CFST columns. This proves that the square and the circular high strength CFST columns exhibit more ductile behaviour peculiarly after the peak load when the $D(H)/t$ ratio is reduced. The average increase in the DI and the SI performance indices for the square and the circular high strength CFST columns, steel tube wall is increased from 3 mm to 5 mm or 6 mm, is 29% and 63%; 38% and 48%, respectively.

The square hollow steel tubes are much more vulnerable to local buckling and much less confinement effect to the concrete core than the circular ones. Hence, the benefit of concrete filling, as indicated by the CCR, is much more critical for the square sections than the circular ones. The average increase in the CCR for the square and the circular high strength CFST columns, steel tube wall reduced from 6 mm or 5 mm to 3 mm, is 41% and 22%, respectively.

The EC4 design code take into account the confinement effect by the steel tube to the concrete core if the relative slenderness does not exceed 0.5 and e/D is smaller than 0.1. The EC4 approach is limited to CFST columns with concrete strength of 50 MPa. Based on the test results, the EC4 overestimate the axial load capacity of the square and the circular high strength CFST columns. However, when the $D(H)/t$ ratio decrease, the EC4 is more conservative and reliable to predict the axial load capacity of the high strength CFST columns. Besides, due to radial expansion of the concrete and, thus, effective confinement by the steel tube to the concrete core occurs in the circular sections, the EC4 is safer for predicting the axial load capacity of the circular high strength CFST columns than the square ones. Furthermore, the EC4 limitation on concrete cylinder strength cannot be safely extended to concrete compressive strength of over 100 MPa. The EC4 may use a reduction coefficient to consider the weak confinement effect of the steel tube to the concrete core and obtain a better agreement with the test results. The biggest difference between the test results and the EC4 for the square and the circular specimens is 37% and 41%, respectively.

The AISC-LRFD is too conservative for predicting the axial load capacity of the square and the circular high strength CFST columns with $D(H)/t$ ratio smaller than 20. However, the predictions of this design code are not safe when the $D(H)/t$ ratio increase. The biggest difference between test results and the AISC-LRFD design codes for the square and the circular specimens is 37% and 46%, respectively.

REFERENCES

- [1] Lu, Z.H. and Zhao, Y.G., "Mechanical Behavior and Ultimate Strength of Circular CFT Columns Subjected to Axial Compression Load", The 14th World Conference on Earthquake Engineering, Beijing, China, 2008.
- [2] Shah, A.A. and Ribakov, Y., "Recent Trends in Steel Fibered High-strength Concrete", *Materials and Design*, 2011, Vol. 32, No. 8-9, pp. 412-415.
- [3] Roeder, C.W., Cameron, B. and Brown, C.B., "Composite Action in Concrete Filled Tubes", *Journal of Structural Engineering*, ASCE, 1998, Vol. 125, No. 5, pp. 477-484.
- [4] Johansson, M. and Gylltoft, K., "Mechanical Behavior of Circular Steel-concrete Composite Stub Columns", *Journal of Structural Engineering*, ASCE, 2002, Vol. 128, No. 8, pp. 1073-1081.
- [5] Giakoumelis, G. and Lam, D., "Axial Capacity of Circular Concrete-filled Tube Columns", *Journal of Constructional Steel Research*, 2004, Vol. 60, No. 7, pp.1049-68.
- [6] Guler, S., Lale, E. and Aydoğan, M., "Behaviour of SFRC Filled Steel Tube Columns under Axial Load", *International Journal of Advanced Steel Construction*, 2013, Vol. 9, No. 1, pp. 14-25
- [7] Eurocode 4 "Design of Composite Steel and Concrete Structures, Part 1.1, General Rules and Rules for Buildings", EN 1994-1-1, European Committee for Standardization: British Standards Institution, 2004.
- [8] American Institute of Steel Construction, AISC, "Load and Resistance Factor Design Specification for Structural Steel Buildings", American Institute of Steel Construction, Chicago, IL, 1999.
- [9] Turkish Standard Institution, TS EN 206. "Concrete-Part 1: Specification, Performance, Production and Conformity", Ankara, Turkey, 2002.
- [10] Turkish Standard Institution, TS EN 12390, "Testing Hardening Concrete- Part 1, Shape, Dimensions and Other Requirements for Specimens and Moulds", Ankara, Turkey, 2002.
- [11] Turkish Standards Institution, TS 138 EN 10002-1, "Metallic Materials – Tensile Testing – Part 1", Ankara, Turkey, 2004.
- [12] Han, L.H., "Tests on Stub Columns of Concrete-filled RHS Sections", *Journal of Constructional Steel Research*, 2002, Vol. 58, No. 2, pp. 353-72.
- [13] Yang, H., Lam, D. and Gardner, L. "Testing and Analysis of Concrete-filled Elliptical Hollow Sections", *Engineering Structures*, 2008, Vol. 30, No. 12, pp. 3771-3781.